

Supporting Information

Industrially Promising Nanowire Heterostructure Catalyst for Enhancing Overall Water Splitting at Large-Current-Density

Guangfu Qian[#], Jinli Chen[#], Lin Luo, Tianqi Yu, Yamei Wang, Wenjie Jiang, Qinglian Xu, Shouqsuan Feng,
Shibin Yin*

Guangxi Key Laboratory of Petrochemical Resource Processing and Process Intensification
Technology, College of Chemistry and Chemical Engineering, School of Physical Science and
Technology, State Key Laboratory of Processing for Non-Ferrous Metal and Featured Materials,
Guangxi University, 100 Daxue Road, Nanning 530004, P. R. China

Total number of pages (including cover page): 14

Total number of Figures: 23

*Corresponding author email: yinshibin@gxu.edu.cn (S. Yin).

[#] These two authors contributed equally to this work.

1. Supplementary Figures

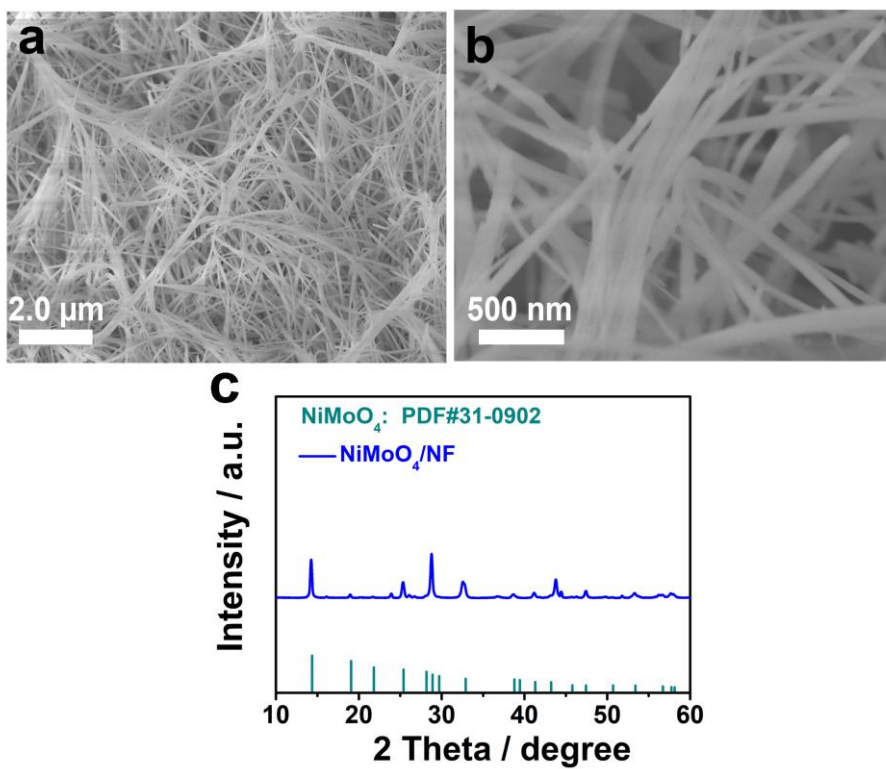


Figure S1. (a, b) SEM and (c) XRD images of the precursors.

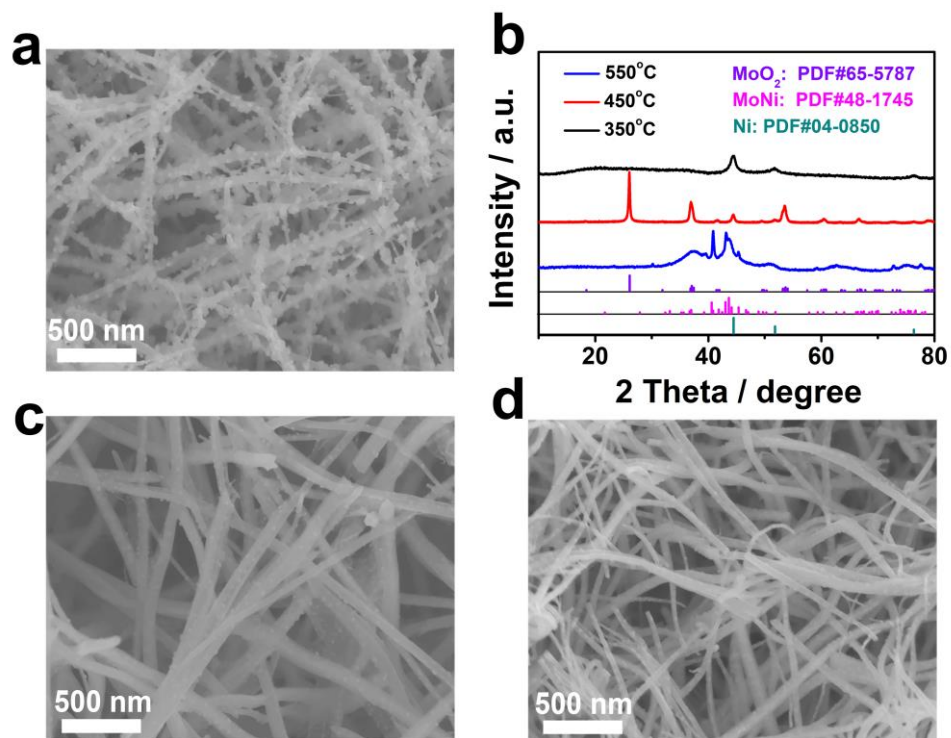


Figure S2. (a, c, d) The precursors are annealed at 450, 350, and 550 °C, respectively; (b) the XRD patterns of the (Ni-MoO₂)@C/NF obtained at different temperatures.

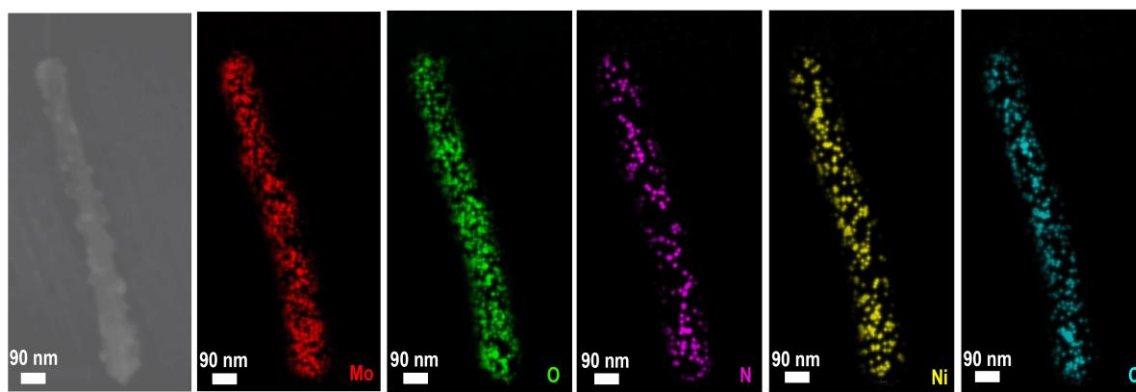


Figure S3. The EDS of SEM mappings after annealed at 450 °C.

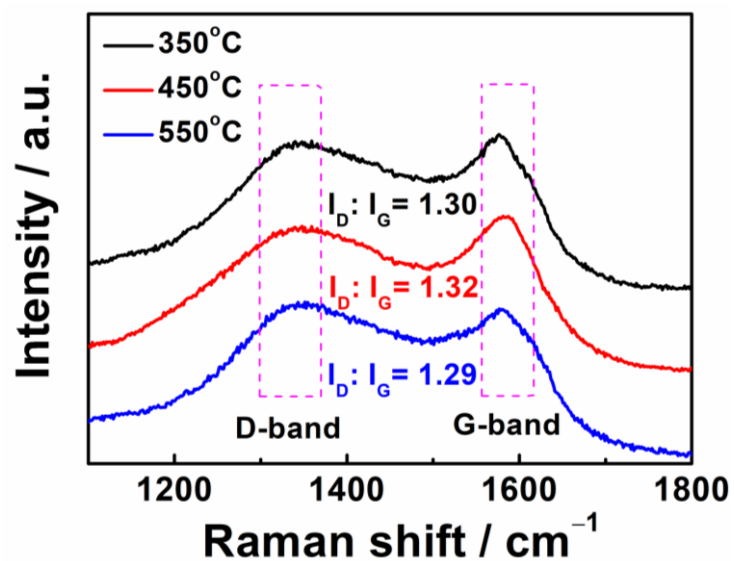


Figure S4. Raman curves of (Ni-MoO₂)@C/NF annealed at different temperatures.

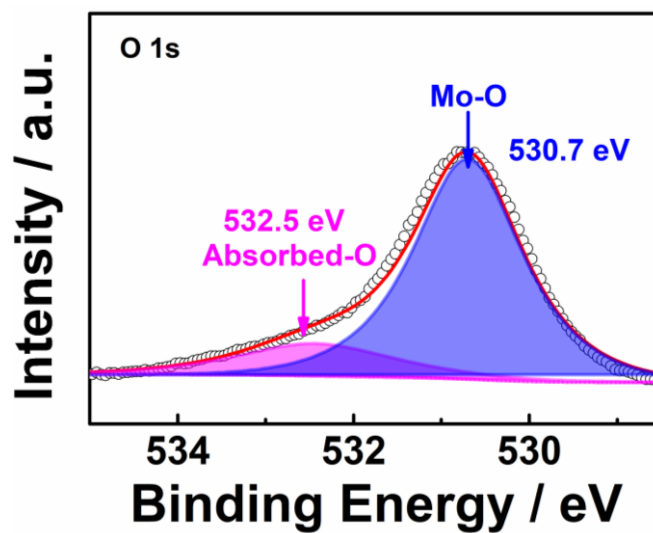


Figure S5. XPS image of (Ni-MoO₂)@C/NF for O 1s.

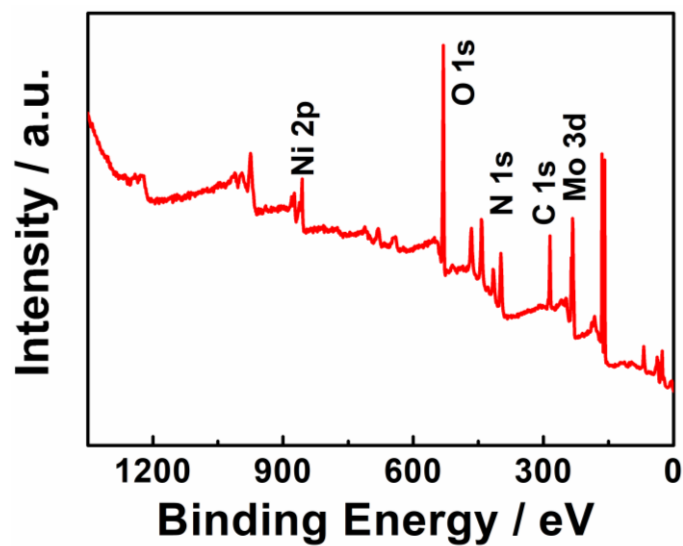


Figure S6. XPS summary spectra of (Ni-MoO₂)@C/NF NWs.

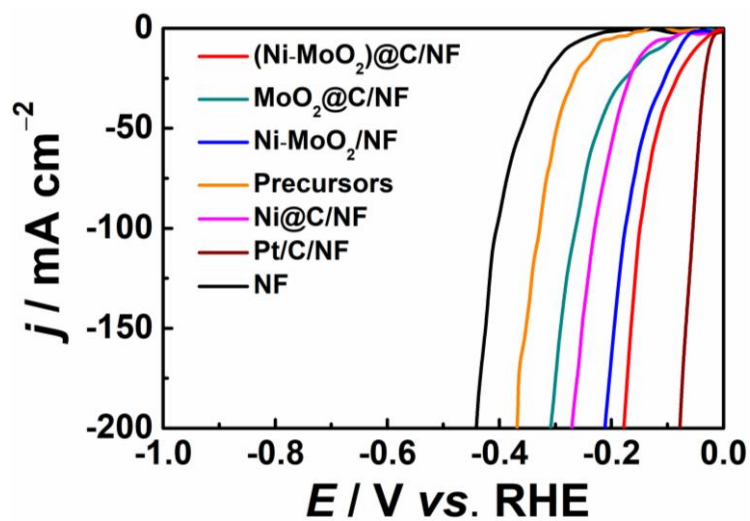


Figure S7. LSV curves for HER of the investigated catalysts in 1.0 M KOH.

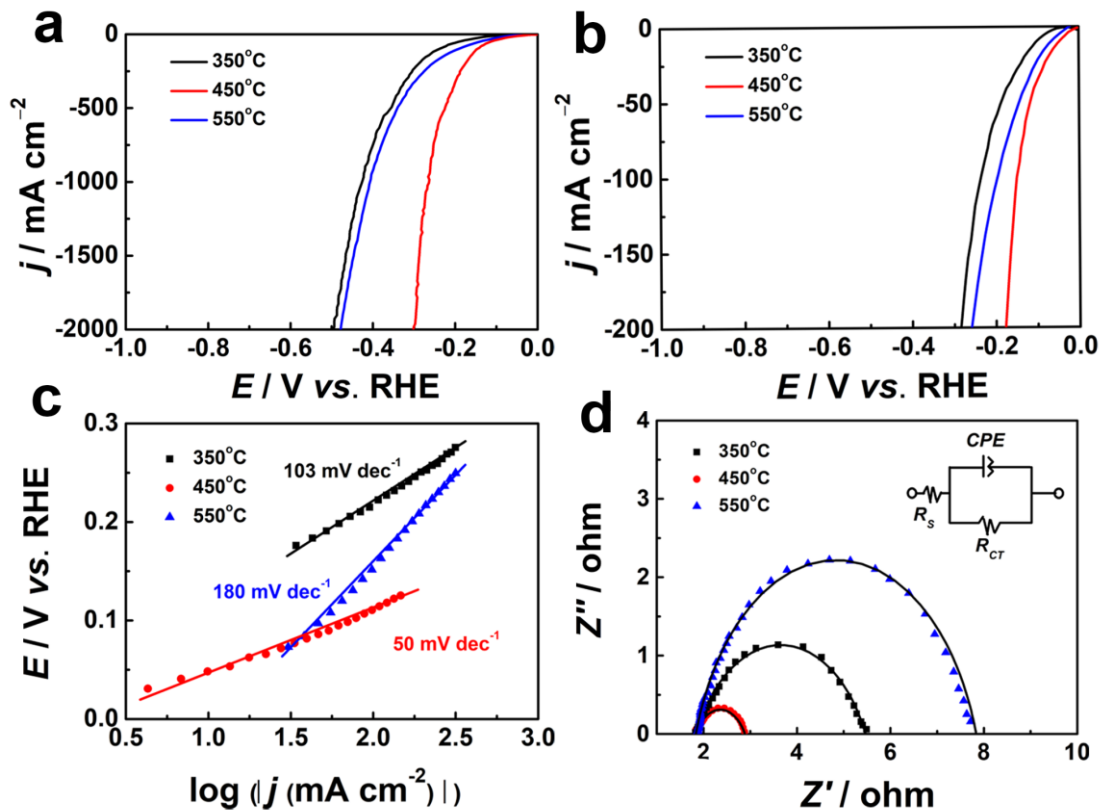


Figure S8. (a, b) LSV curves for HER of (Ni-MoO₂)@C/NF at different temperatures; (c) corresponding Tafel slopes; (d) corresponding Nyquist plots tested at -0.20 V for HER with a frequency from 100 kHz to 100 mHz in 1.0 M KOH; inset is the equivalent circuit model.

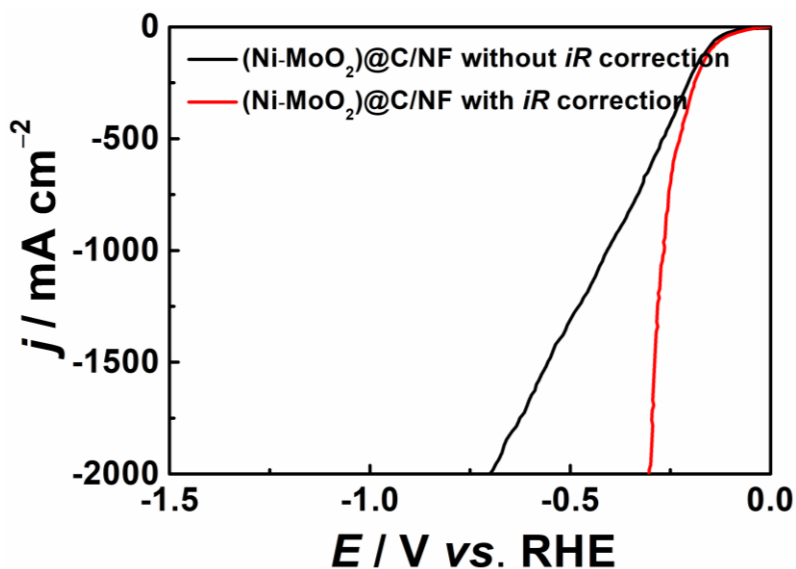


Figure S9. LSV curves of (Ni-MoO₂)@C/NF with/without iR correction for HER.

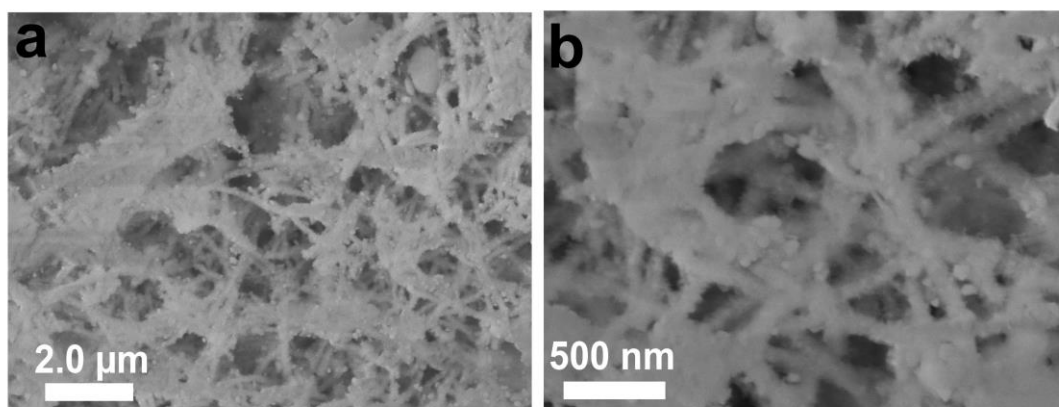


Figure S10. (a, b) SEM images of (Ni-MoO₂)@C/NF after hydrogen evolution stability test.

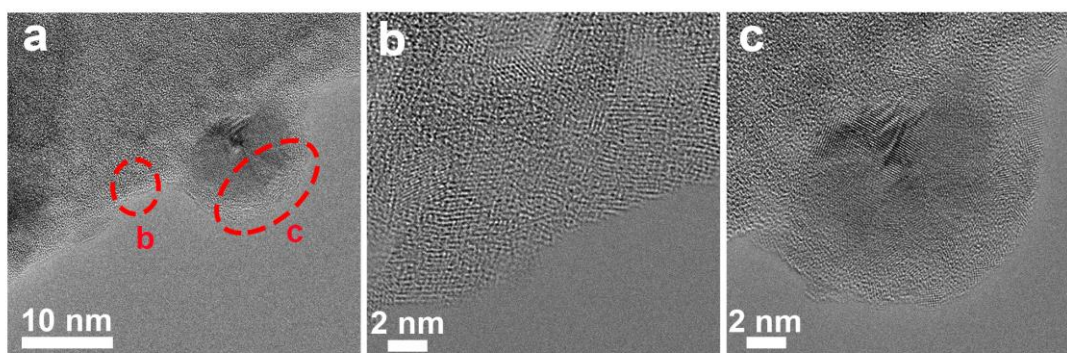


Figure S11. (a-c) TEM images of (Ni-MoO₂)@C/NF after hydrogen evolution stability test.

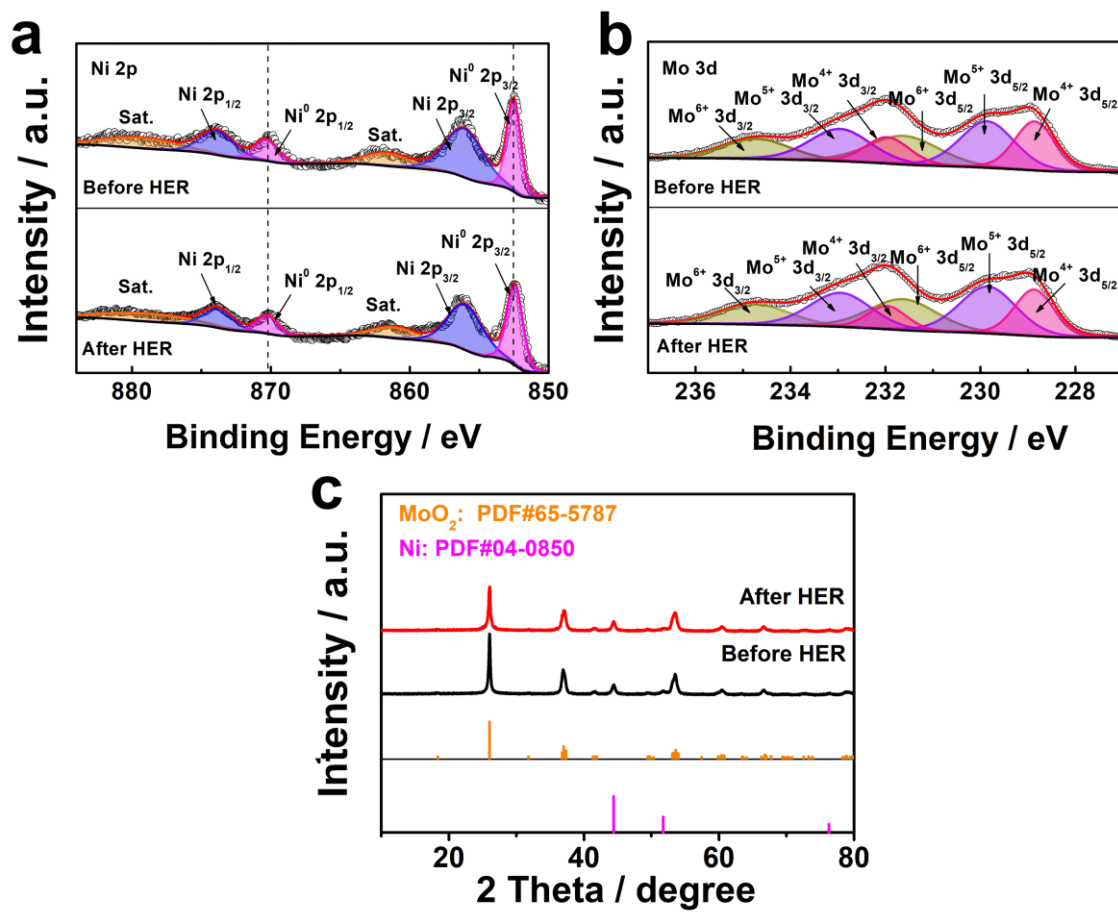


Figure S12. (a, b) XPS and (c) XRD images of (Ni-MoO₂)@C/NF after hydrogen evolution stability test.

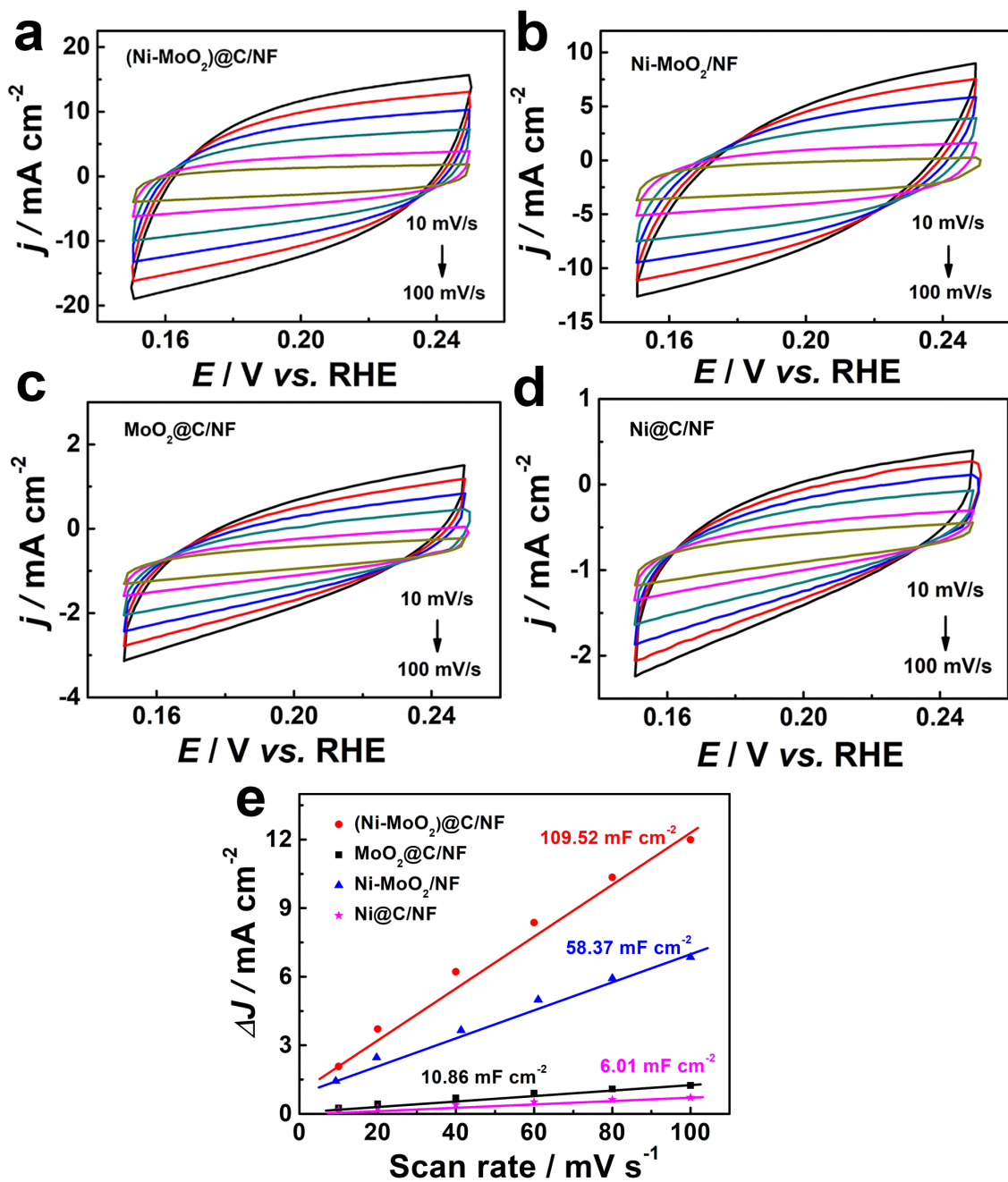


Figure S13. (a-d) Typical cyclic voltammograms of (Ni-MoO₂)@C/NF, Ni-MoO₂/NF, MoO₂@C/NF, and Ni@C/NF at scan rates ranging from 10 to 100 mV s⁻¹, the scanning potential range is from 0.15 V to 0.25 V; (e) estimation of C_{dl} by plotting the capacitive current density against the scan rate to fit a linear regression of the as-prepared samples.

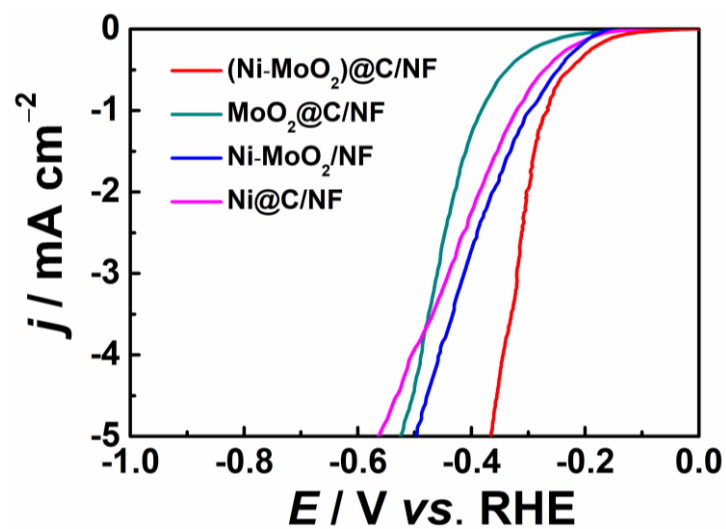


Fig. S14. HER activity (current density) of the samples normalized by their EASAs.

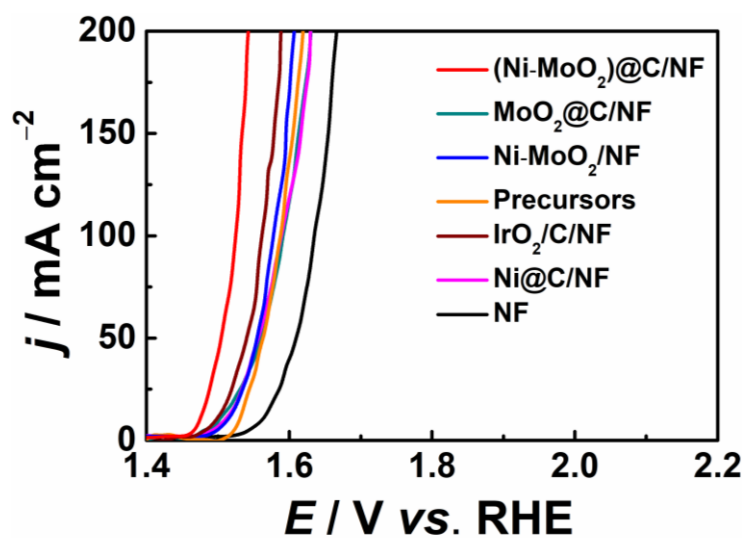


Figure S15. LSV curves of OER for the investigated catalysts in 1.0 M KOH.

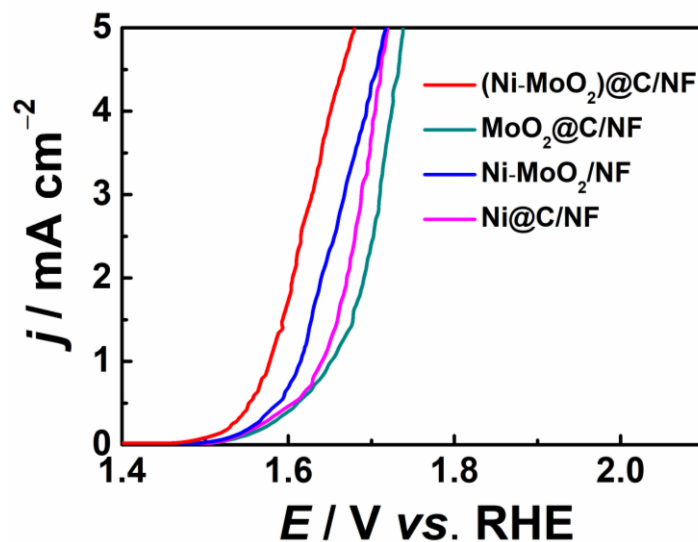


Fig. S16. OER activity (current density) of the samples normalized by their EASAs.

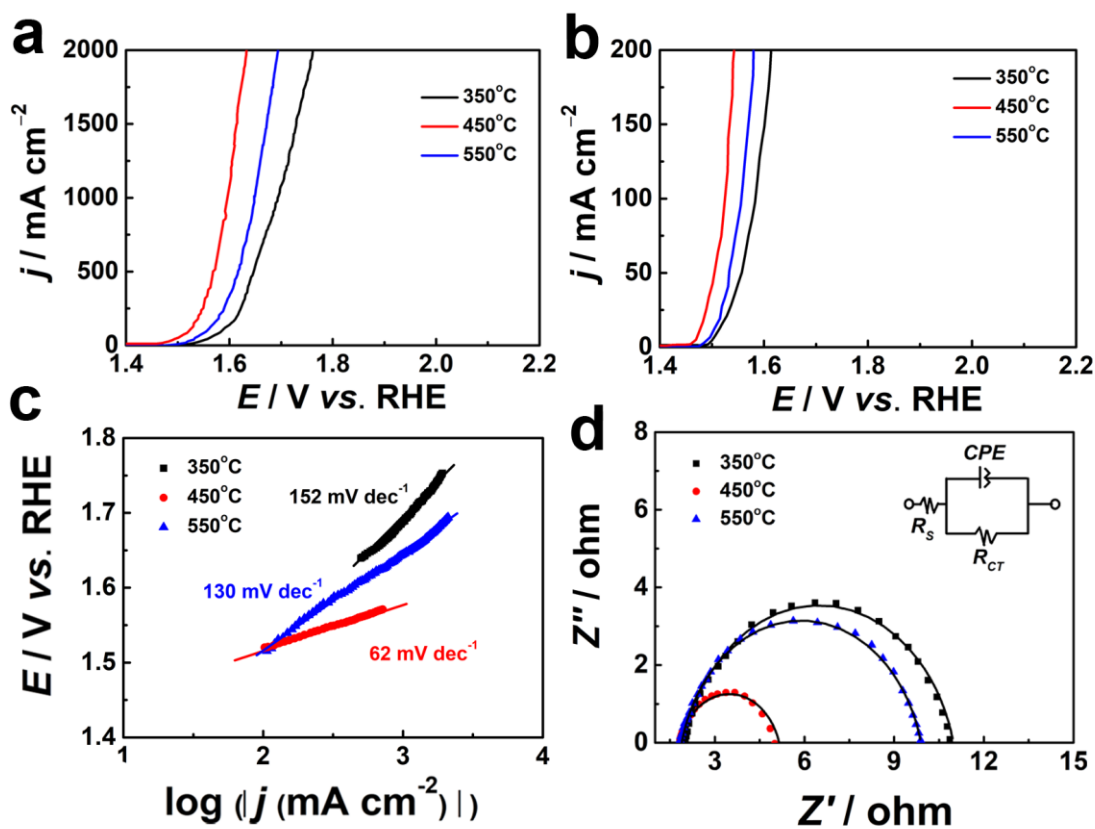


Figure S17. (a, b) LSV curves for OER of (Ni-MoO₂)@C/NF at different temperatures. (c) corresponding Tafel slopes; (d) corresponding Nyquist plots tested at 1.50 V for OER with a frequency from 100 kHz to 100 mHz in 1.0 M KOH; inset is the equivalent circuit model.

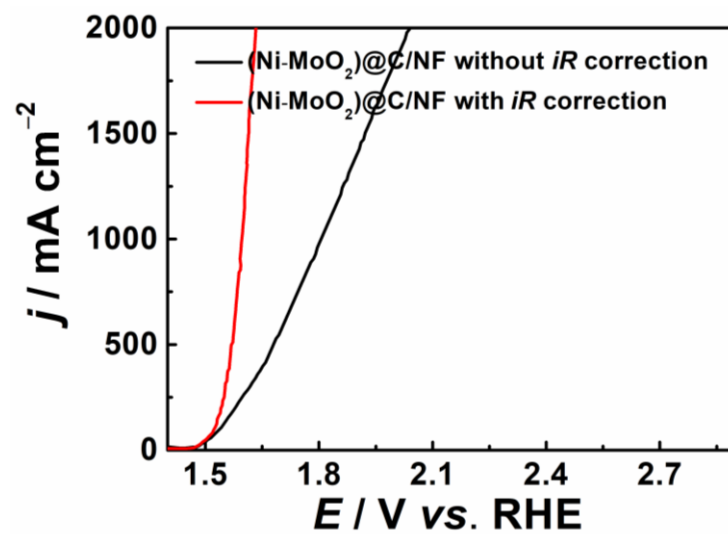


Figure S18. LSV curves of (Ni-MoO₂)@C/NF with/without *iR* correction for OER.

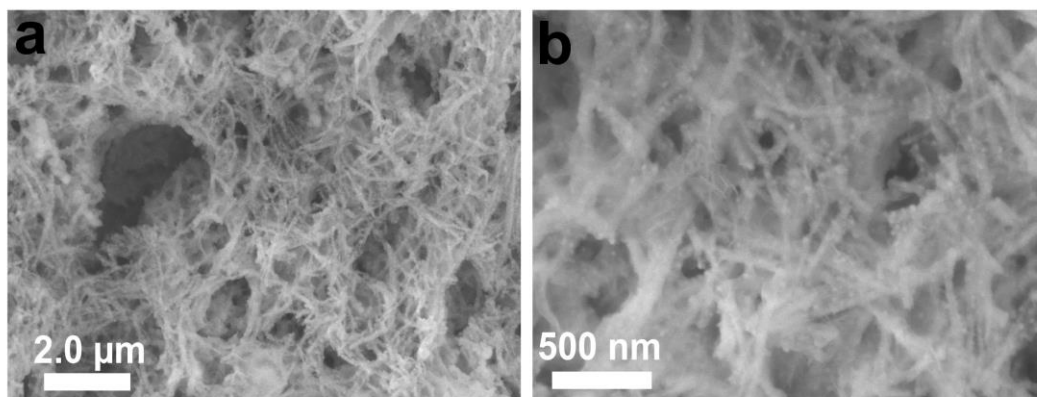


Figure S19. (a, b) SEM images of (Ni-MoO₂)@C/NF after oxygen evolution stability test.

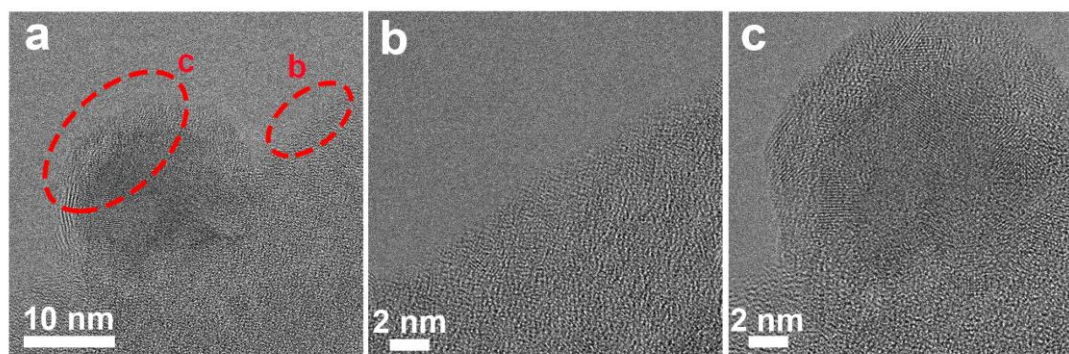


Figure S20. (a-c) TEM images of (Ni-MoO₂)@C/NF after oxygen evolution stability test.

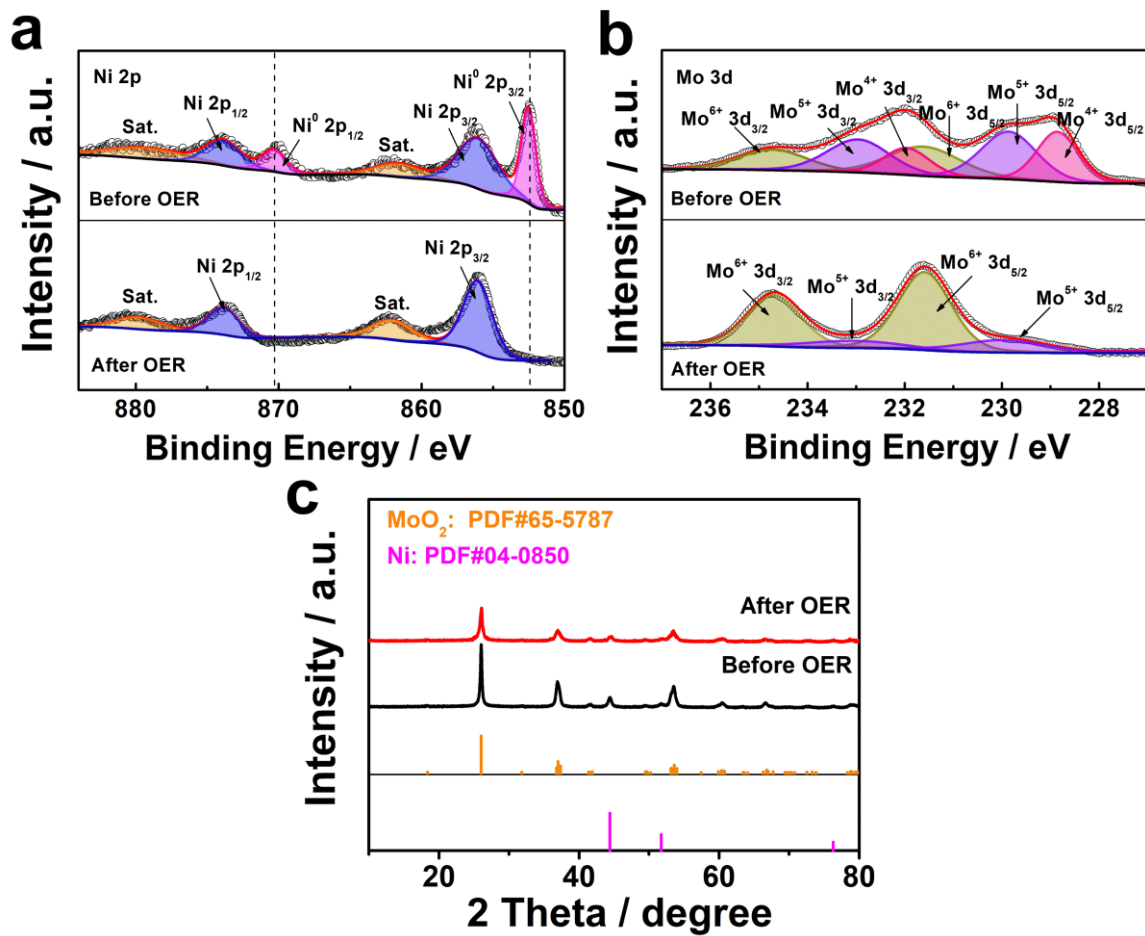


Figure S21. (a, b) XPS and (c) XRD images of (Ni-MoO₂)@C/NF after oxygen evolution stability test.

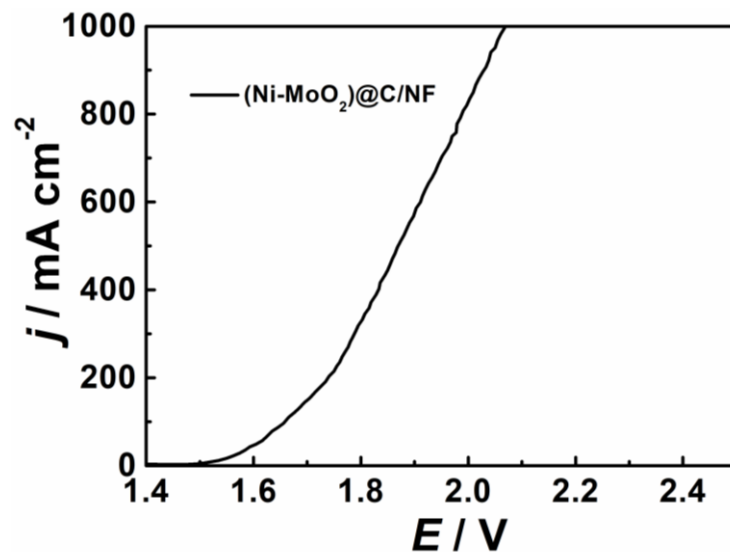


Figure S22. The LSV curves of (Ni-MoO₂)@C/NF || (Ni-MoO₂)@C/NF for overall water splitting.

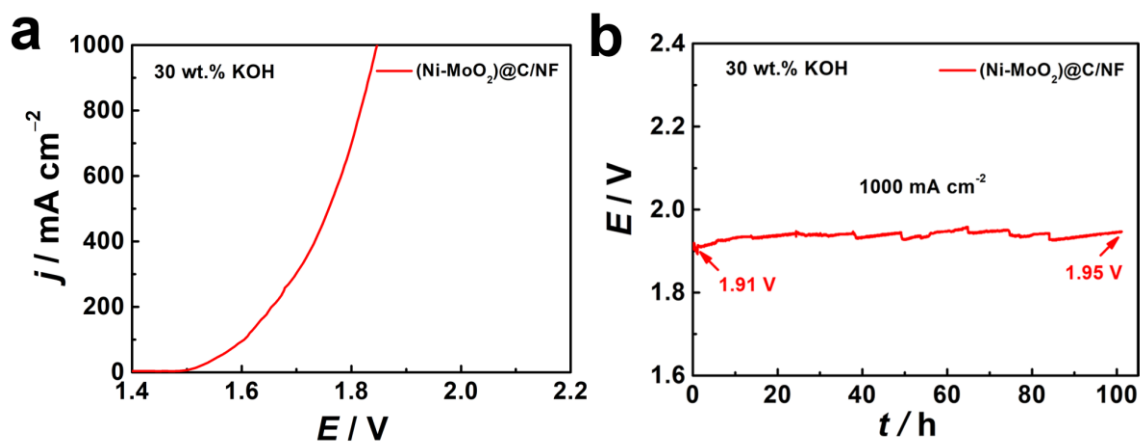


Figure S23. (a) The LSV and (b) stability curves of (Ni-MoO₂)@C/NF || (Ni-MoO₂)@C/NF in 30 wt.% KOH solution for overall water splitting.